

Article

Application of SWASH to Compute Wave Overtopping in Ericeira Harbour for Operational Purposes

Anika Manz ^{1,*}, Ana Catarina Zózimo ^{1,*} and Juan L. Garzon ^{2,*} 

¹ Laboratório Nacional de Engenharia Civil (LNEC), 1700-111 Lisboa, Portugal

² CIMA—Centre for Marine and Environmental Research, Universidade do Algarve, 8005-139 Faro, Portugal

* Correspondence: a67280@ualg.pt (A.M.); aczozimo@lnec.pt (A.C.Z.); jlhervas@ualg.pt (J.L.G.)

Abstract: This work aimed at testing the capability of the numerical model SWASH to be implemented in the prototype of the overtopping and flooding forecast system HIDRALERTA for Ericeira harbour. In contrast to the neural network NN_OVERTOPPING2, which is currently implemented in HIDRALERTA, SWASH is able to estimate the flood extension and wave propagation along the domain, which makes it a possible improvement to NN_OVERTOPPING2. The one-dimensional version of the SWASH model was implemented to simulate overtopping at two different profiles (antifer and tetrapods) and calibrated for three storms in 2019 by comparing the simulated overtopping discharge to NN_OVERTOPPING2 results. For the calibration, the Manning coefficient was used to represent the friction of the armour layer. Then, for operational purposes, four expressions to calculate the Manning coefficient were developed based on: the relative crest freeboard, the wave steepness, the incident wave angle and the type of armour layer. The expressions showed small errors between the calculated and calibrated Manning coefficients and highlighted the importance of the incident wave angle to obtain an accurate calibration. Despite an underestimation of the overtopping discharge in some cases, the SWASH model was found to provide overall good results when applied with calculated Manning coefficients and suitable to be implemented in HIDRALERTA.

Keywords: wave overtopping; early warning system; SWASH; Manning coefficient; HIDRALERTA; To-SEAlert



Citation: Manz, A.; Zózimo, A.C.; Garzon, J.L. Application of SWASH to Compute Wave Overtopping in Ericeira Harbour for Operational Purposes. *J. Mar. Sci. Eng.* **2022**, *10*, 1881. <https://doi.org/10.3390/jmse10121881>

Academic Editor: Barbara Zanuttigh

Received: 22 October 2022
Accepted: 28 November 2022
Published: 3 December 2022

Publisher's Note: MDPI stays neutral with regard to jurisdictional claims in published maps and institutional affiliations.



Copyright: © 2022 by the authors. Licensee MDPI, Basel, Switzerland. This article is an open access article distributed under the terms and conditions of the Creative Commons Attribution (CC BY) license (<https://creativecommons.org/licenses/by/4.0/>).

1. Introduction

Adverse sea conditions can result in wave-induced overtopping and flooding, having a negative impact on society, the environment and economy [1,2]. In many regions, coastal communities and socio-economic activities rely on the capability of coastal structures to minimise the consequences of wave-induced flooding. Yet, these structures are rarely designed for zero overtopping discharges [3]. To reduce the risks caused by these hazards, forecast and early warning systems (EWSs) have been identified as an important tool to detect emergency situations and to initiate the necessary safety measures [4]. While the United Nations calls to strengthen these prediction systems, they are still in their infancy. In Europe, only some efforts have been made to implement EWSs (e.g., [5,6]) and in many countries such as Portugal, highly exposed to coastal hazards, no fully operational national flood forecast and early warning system exists yet.

The HIDRALERTA system [7–11] aims to contribute to filling this gap. HIDRALERTA is a wave overtopping and flooding forecast system with early warning and risk assessment capabilities. It runs in real-time mode and enables the identification of emergency situations in coastal and harbour areas with 72 h of anticipation. The system uses a neuronal network system, NN_OVERTOPPING2 [12], to compute mean overtopping discharge q at several cross-sections of the structure in harbour areas. NN_OVERTOPPING2 uses as input conditions the results of the numerical wave propagation model DREAMS [13] and tide levels from the XTIDE model [14]. Warnings are triggered when pre-set thresholds for q are exceeded and forecasts are sent daily to decision-makers [2,7,8].

While wave overtopping has been traditionally estimated through physical modelling or with (semi-) empirical formulas (e.g., [15,16]), advances in computer hardware and numerical methods in recent years have made it possible to use numerical models to obtain accurate estimations of physical processes such as wave propagation and transformation in shallow areas and overtopping over the defense structures [17].

A recent approach to model wave overtopping is based on the dispersive NLSW (Non Linear Shallow Water) equations, which include a non-hydrostatic pressure term, as well as a resolution of the vertical flow and its structure. The SWASH model (an acronym for Simulating WAVes till SHore) [18] numerically simulates non-hydrostatic, free-surface, rotational flows in one or two horizontal dimensions. As the governing equations rely on the NLSW equations and include non-hydrostatic pressure, they can describe complex and rapidly changing flows in detailed topo-bathymetries that are often found in coastal flooding events. Previous studies have demonstrated the good skills of the model in simulating wave propagation in shallow conditions and wave overtopping discharge [17,19–23].

This study was developed within the frame of the To-SEAlert project, which aims at increasing the reliability and accuracy of HIDRALERTA. The main objective of this study was to investigate the suitability of the numerical model SWASH to be integrated into the HIDRALERTA system for the Ericeira harbour. The SWASH model is considered a robust process-based model with high accuracy of simulating wave propagation in shallow water [16]. Given that any point in the numerical domain can be specified in the output of the SWASH model, it is possible to estimate the inland incursion of overtopping discharges or, in the case of two-dimensional models, the flooded area, as well as the wave propagation along the domain, which the neural network tool NN_OVERTOPPING2, the current approach implemented in HIDRALERTA, is not capable of. In order to achieve this objective, a one-dimensional model was implemented for two profiles of Ericeira breakwater, where the model was applied to simulate overtopping during storm conditions. Its results for mean overtopping discharge were compared to NN_OVERTOPPING2. The main efforts were devoted to calibrating the model by varying the Manning coefficient that represents the friction of the armour layer of the breakwater and to get the best agreement with the overtopping estimations obtained from NN_OVERTOPPING2. For predictive purposes, expressions for the determination of the Manning coefficient were derived, allowing to simulate wave-induced flooding during storms for a given type of armour layer. These expressions are of capital importance for the successful implementation of a numerical model into a real-time forecast system, since its parameterisation has to be previously and seamlessly defined based on some oceanic and site-specific conditions of the case.

2. Materials and Methods

2.1. Study Site

Ericeira harbour is located on the west coast of Portugal. It is sheltered by a 430 m long breakwater, oriented to the south-west, with a quay in the rear side. For the simulation of wave overtopping, two profiles were chosen. Profile-A has an armour layer of antifer cubes and is located at the head of the breakwater. It has an orientation of 262° N. Profile-T consists of tetrapods and is in the vicinity of the quay of the breakwater and has an orientation of 309° N (Figure 1).

The two profiles differ in their slope angle, their crest freeboard R_c and armour freeboard A_c and in the width of the crest G_c (Table 1).

Table 1. Structure characteristics of the breakwater profiles referred to the Portuguese hydrographic zero (ZH).

	Slope	R_c (m)	A_c (m)	G_c (m)
Profile-A	1:2.0	9.03	10.85	5.79
Profile-T	1:1.5	8.98	10.20	5.28

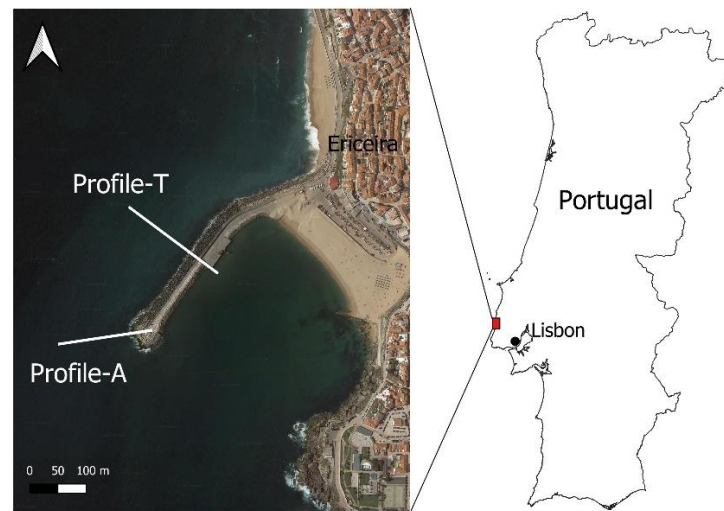


Figure 1. Location of Ericeira harbour and the breakwater profiles.

The simulations were performed for three consecutive storms that hit the study area between the 15th and 23rd of December 2019 (Figure 2). The first storm occurred between the 15th and 17th and remained unnamed, with wave directions between 280° and 300° N, a maximum peak period T_p of 16.7 s and a maximum significant wave height H_s of 5.57 m. The Elsa storm occurred from 19th to 21st of December and had wave directions between 260° and 280° N, maximum T_p of 13.6 s and maximum H_s of 7.93 m. The Fabien storm hit the study area between 22nd and 23rd of December and had wave directions between 257° and 290° N, maximum T_p of 16.7 s and maximum H_s of 7.14 m.

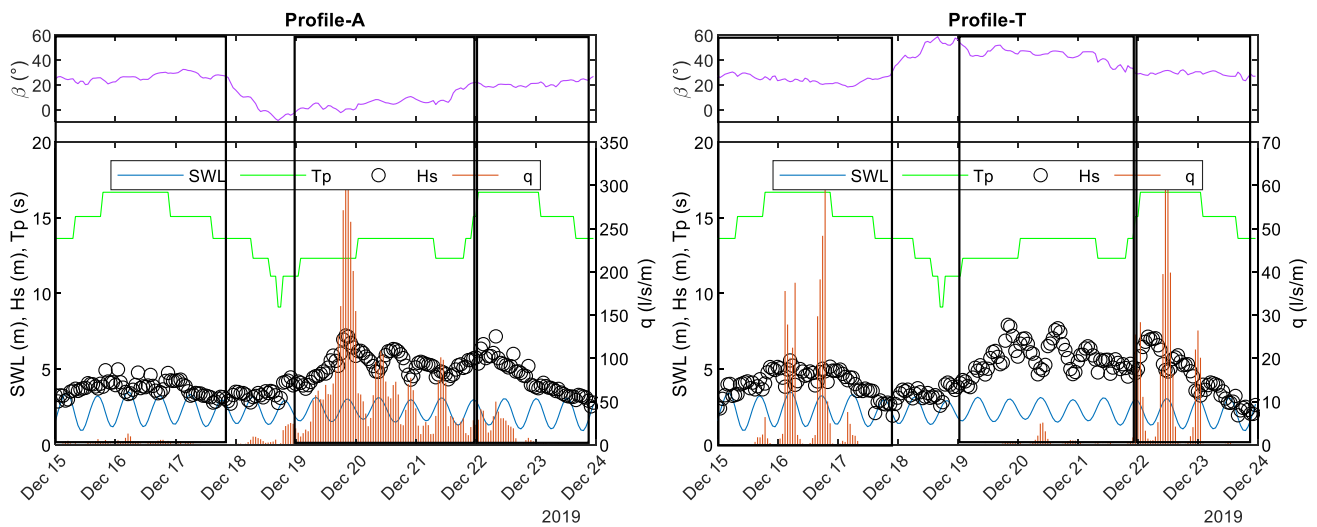


Figure 2. Time series of the simulated storms of Profile-A and Profile-T (from left to right). The boxes indicate the first storm (unnamed), the Elsa storm and the Fabien storm. SWL indicates the Still Water Level, q is the mean overtopping discharge and β ($^\circ$) is the angle of wave attack, which is the angle between the incident wave direction and the perpendicular to the profile.

The oceanic offshore conditions (waves, wind and surge) during these storms were obtained from ERA-5 hindcast data downloaded from the Copernicus Climate Change Service (C3S) Climate Data Store [24]. This information was then introduced in the numerical framework developed for HIDRALERTA. This framework uses the XTIDE model [14] for the astronomical tide data, and the models SWAN [25] and DREAMS [13] to propagate the wave conditions from offshore to the vicinity of the structure. To force the SWASH models, water levels and wave regimes were extracted at the points located at the offshore boundary

of the simulated profiles (341 m distance of the breakwater with a depth of 14.47 m below the Portuguese hydrographic zero, ZH, for Profile-A and 335 m distance of the breakwater with a depth of 9.5 m ZH for Profile-T). In addition, to compare with the performance of the actual HIDRALERTA system, oceanic conditions were extracted at the toe of the structure and used on NN_OVERTOPPING2 to compute the overtopping discharge. The overtopping discharges were calculated with a 1-h time step.

2.2. SWASH Model Setup

Simulations were performed in a one-dimensional mode for a computational period corresponding to 500 waves, with an additional spin-up period of 15% of the computational period. While the SWASH user manual recommends between 500 and 1000 waves for a steady-state resolution, the minimum was applied for a low computational cost. An initial timestep of 0.008 s and an automatic time step control was applied with a maximum Courant number of 0.5 and a minimum Courant number of 0.1. The number of vertical layers used for the simulations was determined by the maximum frequency of each case, which resulted in one vertical layer for all simulations. Considering that the SWASH user manual sets the default Manning friction coefficient to 0.019 s/(m^{1/3}) for wave simulations over large distances, a minimum value of 0.02 s/(m^{1/3}) was imposed for the calibration of the model for the armour layers of the breakwater, as the tetrapods and antifer cubes likely cause higher friction than found in the approximation area.

Profile-A had a domain length of 392 m, where 341 m corresponded to the approximation area and 51 m to the breakwater. The length of the numerical domain was 419 m for profile-T, where 334.5 m corresponded to the approximation area, 48 m to the breakwater and 36.5 m to the lee side of the structure (Figure 3). The length of the SWASH computational domains was a consequence of the depth needed to comply with the model requisites at the offshore boundary in terms of the relation between water depth and significant wave height and between water depth and mean wave period. The bathymetry was constructed with data acquired from EMODnet (150 m grid spacing) and DGTerritorio (LiDAR survey of 2011, 2 m spacing). The profiles had a constant grid spacing of 0.5 m. Mean overtopping discharge, *q*, was defined at the red markers in Figure 3 by simulating the instantaneous overtopping discharge at each time step using the DISCH command in SWASH. In order to obtain the mean overtopping discharge, the sum of discharges was divided by the computational time (or the amount of instantaneous discharges that was received in the output).

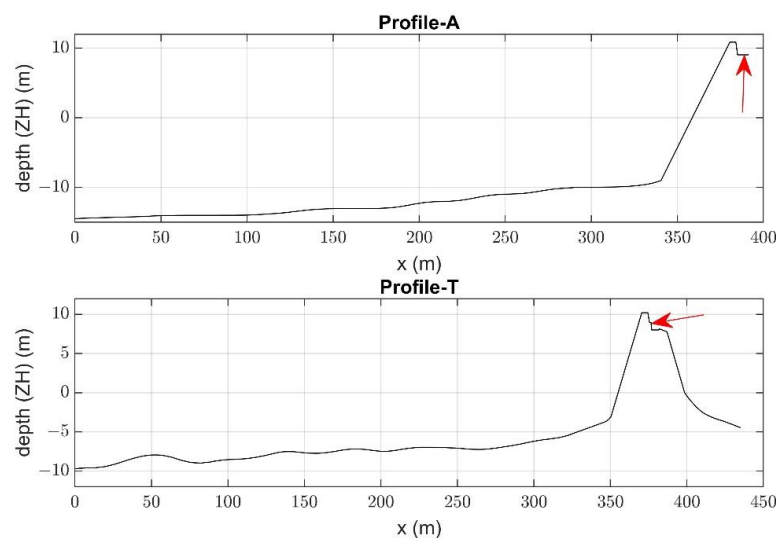


Figure 3. Bathymetries used for the simulations in SWASH, with the cross-shore distance referred to the wavemaker boundary and red arrows indicating where overtopping results were extracted.

At the offshore boundary, a Jonswap wave spectrum defined the shape of the irregular waves, with a peak enhancement parameter $\gamma = 3.3$, and a weakly-reflective boundary

was imposed. A Sommerfeld radiation boundary condition was applied at the end of the domain to prevent the reflection of outgoing waves that could give rise to instabilities within the numerical domain. The boundary conditions were chosen based on several existing overtopping studies [17,20]. For the non-hydrostatic pressure term, a Keller Box scheme with ILU preconditioner was used to increase the stability of the model.

2.3. Model Calibration

A possible approach to simulate wave overtopping over a breakwater is to define the breakwater in terms of the porosity of its material. However, previous studies showed that the use of a porosity term may lead to wave dissipation without wave run-up and overtopping [26,27]. Alternatively, a permeable breakwater can be treated as impermeable terrain using a bottom friction coefficient, which represents the effect of comprehensive energy dissipation as a consequence of roughness [26]. So, in this study, the friction and rugosity of the breakwater was included in the form of a Manning coefficient, which is also a simpler approach to implement in operational systems like HIDRALERTA. As the literature does not provide a friction value or a Manning coefficient for tetrapods or antifer cubes, the model was calibrated by varying Manning values in order to obtain discharges similar to the ones estimated by HIDRALERTA by using the NN-OVERTOPPING2 tool. This way, the effect of porosity was accounted for in the calibration of the Manning coefficient. The neural network NN_OVERTOPPING2 was developed as part of the CLASH European project and based on a large database of physical model tests for a wide range of coastal structure types. Therefore, the mean overtopping discharge of the antifer and tetrapod armoured breakwater for the calibration was provided by the NN_OVERTOPPING2 neural network. NN_OVERTOPPING2 uses a roughness and permeability coefficient, provided in [28], depending on the type of armour layer.

Following the results of [21], who found a correlation of the friction coefficient with the wave steepness S_{op} (wave height H /wavelength λ) and the relative crest freeboard R_c/H_s , the cases were chosen to account for a wide range of S_{op} and R_c/H_s conditions, where the crest freeboard R_c defines the height of the superstructure relative to SWL. Given that it is not possible to account for wave direction in one-dimensional simulations and that NN_OVERTOPPING2, in contrast, does account for wave direction in overtopping estimations, the cases were also sorted according to their incident wave angles β above and below 15° . The main reason for this is that oblique wave attack reduces the overtopping discharge estimated by NN_OVERTOPPING2 and that SWASH can replicate this in the form of a higher Manning friction coefficient, resulting in lower discharges. The threshold of 15° was chosen based on the studies of [29], who found that there is no significant difference in overtopping for wave attack over an armoured breakwater between 0 and 15° .

Twenty-four simulations were performed for profile-T, which included sea states from the three different storms, where β varied between 18° and 49° . The values for wave steepness ranged from 0.02 to 0.05 and for dimensionless crest freeboards between 1.0 and 1.9. Profile-A was almost aligned with the dominant wave direction that occurred during the Elsa storm (β lower than 15° , representing normal wave attack). Twelve cases were simulated from this storm with incident wave angles below 15° , wave steepness values ranging from 0.02 to 0.05 and dimensionless crest freeboards between 1.1 and 2.1.

2.4. Manning Coefficient Expression Development and Validation

Following the study from [21], the relation of both wave steepness and relative crest freeboard with overtopping discharges and the Manning coefficients obtained in the calibration process ($n_{calibrated}$) were investigated. Then, for predictive purposes, empirical equations to obtain $n_{calculated}$ as a function of the hydrodynamic conditions and the geometry of the structure were developed. To develop these equations, the Matlab CFtool was utilised to find the best fitting using least square regression. To evaluate the accuracy of the empirical equations, discharges computed with $n_{calibrated}$ were confronted with the discharges

computed with $n_{calculated}$ along with the discharges provided by NN_OVERTOPPING2 by using the Root-Mean-Square-Error (RMSE).

For Profile-A, based on the chosen cases (Table 2), one equation was developed:

- Equation (1)—defining n_A as a function of R_c/H_s and S_{op} , where n_A is the Manning coefficient of an armour layer of antifer cubes. This equation does not account for wave obliquity and can only be applied under normal wave attack conditions, i.e., incident angles lower than 15° .

Table 2. Cases chosen for SWASH simulations for profile-A with wave characteristics from the Elsa storm.

Case No	Date and Time	R_c/H_s	S_{op}	H_s (m)	T_p (s)	SWL (m)	Incident Wave Angle β ($^\circ$)
1	19 December 2019, 18:00	1.10	0.05	6.03	12.33	2.39	2.00
2	20 December 2019, 01:00	1.10	0.04	6.19	13.64	1.97	5.00
3	20 December 2019, 03:00	1.20	0.04	6.07	13.64	1.68	5.00
4	20 December 2019, 07:00	1.20	0.03	5.20	13.64	2.70	8.00
5	19 December 2019, 15:00	1.30	0.05	5.90	12.33	1.55	2.00
6	19 December 2019, 10:00	1.30	0.04	4.68	12.33	2.77	3.00
7	19 December 2019, 11:00	1.40	0.04	4.85	12.33	2.39	0.40
8	21 December 2019, 08:00	1.40	0.03	4.46	12.33	2.59	4.00
9	18 December 2019, 22:00	1.50	0.04	4.45	11.14	2.45	4.00
10	19 December 2019, 06:00	1.50	0.03	4.15	12.33	2.76	3.00
11	19 December 2019, 00:00	1.80	0.04	4.03	11.14	1.80	2.00
12	19 December 2019, 02:00	1.80	0.03	4.10	12.33	1.58	1.00
13	18 December 2019, 10:00	2.10	0.03	3.28	12.33	2.28	1.00
14	18 December 2019, 05:00	2.10	0.02	2.95	13.64	2.79	11.00

For Profile-T, firstly, the 24 simulations for the time period between the 15th and 23rd of December 2019 were considered. Secondly, given that the SWASH model does not take wave direction into account for one-dimensional simulations, the importance of the wave angles β was investigated as well. The 24 simulations were separated into two incident wave climates. Wave climate 1 was characterised by lower wave steepness and β between 15° and 30° . Wave climate 2 showed higher values for wave steepness and waves approached the structure with β between 30° and 50° (Table 3). This way, it was possible to investigate whether or not the performance of the expression to define the Manning coefficient depends on the specific wave conditions that were used to build the expression. Thus, for Profile-T, three equations for the calculation of the Manning coefficient were developed for different ranges of wave attack angles:

- Equation (2)—defining $n_{T,oblique}$ as a function of R_c/H_s and $\cos(\beta)$, where $n_{T,oblique}$ is the Manning coefficient for a tetrapod armour layer. This equation accounts for obliquity and is only applicable to oblique wave attack with incident angles greater than 15° . For that, the 24 cases were considered.
- As an alternative to Equation (2), the following Equations can be used, depending on the incident wave angle:
- Equation (3)—defining $n_{T,oblique(15-30)}$ as a function of R_c/H_s and S_{op} , where $n_{T,oblique(15-30)}$ is the Manning coefficient for a tetrapod armour layer for wave attack between 15° and 30° , based on the data from wave climate 1.
- Equation (4)—defining $n_{T,oblique(30-50)}$ as a function of R_c/H_s and S_{op} , where $n_{T,oblique(30-50)}$ is the Manning coefficient for a tetrapod armour layer for wave attack between 30° and 50° , based on the data from wave climate 2.

Table 3. Cases chosen for SWASH simulations for Profile-T with wave characteristics from the three storms. Separation of cases for the tetrapod profile for wave climate 1 (framed) and wave climate 2 (not framed).

Case No	Date and Time	R_c/H_s	S_{op}	H_s (m)	T_p (s)	SWL (m)	Incident Wave Angle β ($^\circ$)
1	16 December 2019. 05:00	1.00	0.03	5.57	16.69	3.50	23.00
2	16 December 2019. 06:00	1.10	0.03	5.23	16.69	3.41	23.00
3	20 December 2019. 06:00	1.10	0.05	6.02	13.64	2.35	45.00
4	20 December 2019. 20:00	1.10	0.04	5.83	13.64	3.06	42.00
5	19 December 2019. 18:00	1.20	0.05	5.43	12.33	2.39	49.00
6	21 December 2019. 07:00	1.20	0.04	5.64	13.64	2.21	45.00
7	16 December 2019. 17:00	1.20	0.03	4.81	16.69	3.21	21.00
8	22 December 2019. 12:00	1.20	0.03	4.84	16.69	3.03	32.00
9	21 December 2019. 14:00	1.40	0.05	5.10	12.33	2.06	32.00
10	21 December 2019. 13:00	1.40	0.04	4.70	12.33	2.49	34.00
11	17 December 2019. 04:00	1.40	0.03	4.27	15.09	2.92	18.00
12	22 December 2019. 22:00	1.40	0.03	4.53	16.69	2.53	30.00
13	21 December 2019. 20:00	1.50	0.04	4.51	13.64	2.14	35.00
14	15 December 2019. 22:00	1.50	0.03	5.02	16.69	1.25	27.00
15	16 December 2019. 07:00	1.50	0.02	3.96	16.69	3.06	25.00
16	15 December 2019. 14:00	1.60	0.03	4.11	15.09	2.35	27.00
17	16 December 2019. 15:00	1.60	0.02	3.93	16.69	2.54	23.00
18	15 December 2019. 15:00	1.70	0.03	3.66	15.09	2.80	26.00
19	17 December 2019. 08:00	1.70	0.02	3.56	15.09	2.83	21.00
20	23 December 2019. 00:00	1.70	0.02	3.53	16.69	3.06	31.00
21	15 December 2019. 03:00	1.80	0.03	3.28	13.64	3.15	29.00
22	15 December 2019. 06:00	1.80	0.02	3.24	13.64	3.07	30.00
23	23 December 2019. 03:00	1.90	0.03	3.63	15.09	2.14	30.00
24	18 December 2019. 06:00	1.90	0.02	3.07	13.64	3.08	42.00

3. Results

3.1. Profile-A

For Profile-A, the mean overtopping discharge simulated by SWASH was, in general, in agreement with the values obtained by NN_OVERTOPPING2 (see Appendix A, Table A1). Only a limited number of cases were found where the discharge computed by SWASH was much lower than the one estimated by NN_OVERTOPPING2 (3, 43, 11 and 10 l/s/m for cases 13, 1, 11 and 5, respectively). However, it is important to note that the overtopping discharges estimated by NN_OVERTOPPING2 ranged from 3 to 160 l/s/m (Appendix A, Table A1). The discrepancies between q simulated by SWASH and q simulated by NN_OVERTOPPING2 yielded an RMSE of 12.11 l/s/m.

When confronting the calibrated Manning coefficients with the dimensionless numbers, an inverse correlation between the Manning coefficient and R_c/H_s and S_{op} was observed, where the Manning coefficient increased when both parameters decreased (Figure 4a). Similarly, the overtopping discharge tended to decrease with increasing R_c/H_s for a specific S_{op} (Figure 4b).

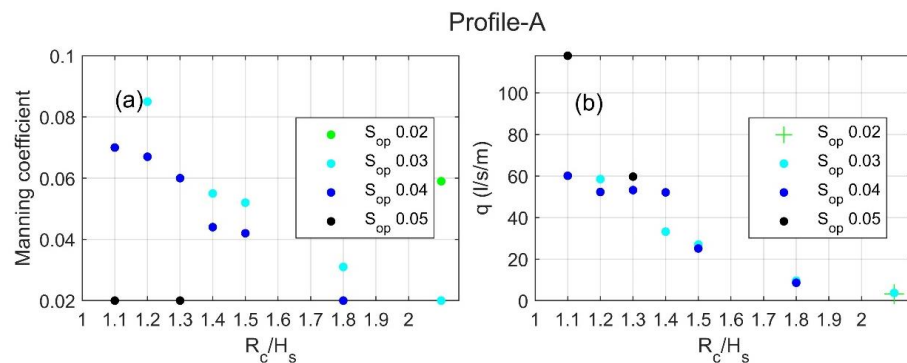


Figure 4. Profile-A. Relation between the Manning coefficient and R_c/H_s (a) and between q and R_c/H_s (b).

Based on these correlations, an empirical equation of the Manning coefficient for an armour layer of antifer cubes as a function of R_c/H_s and S_{op} was developed for wave attack angles smaller than 15° . The equation of the Manning coefficient n_A ($s/m^{1/3}$) was given as follows:

$$n_A = a1 + a2 \times R_c/H_s + a3 \times S_{op} + a4 \times (R_c/H_s)^2 + a5 \times R_c/H_s \times S_{op} + a6 \times S_{op}^2 + a7 \times (R_c/H_s)^3 + a8 \times (R_c/H_s)^2 \times S_{op} + a9 \times R_c/H_s \times S_{op}^2 + a10 \times S_{op}^3 \tag{1}$$

where $a1 = 1.149$; $a2 = -1.402$; $a3 = -22.96$; $a4 = 0.5556$; $a5 = 22.77$; $a6 = 166.5$; $a7 = -0.0453$; $a8 = -8.814$; $a9 = 73.37$; $a10 = -3105$.

The range of application for Equation (1) was between 1.1 and 2.1 for R_c/H_s and between 0.02 and 0.05 for S_{op} (see Appendix B, Figure A1). The Manning coefficients calculated with the equation showed good agreement with the Manning coefficients that were calibrated in the previous sections for each case (Figure 5). According to these results, RMSE between the 14 calibrated and calculated Manning coefficients was $0.002 s/(m^{1/3})$.

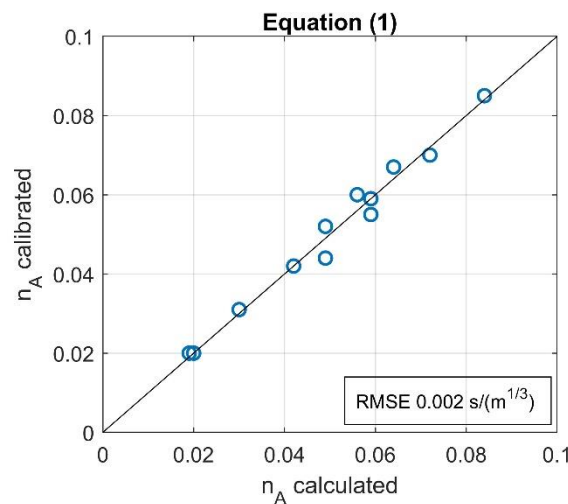


Figure 5. Profile-A. Comparison of calibrated Manning coefficients ($s/(m^{1/3})$) with the ones calculated with Equation (1).

When the calculated Manning coefficient was used to simulate the overtopping discharge with SWASH for the 14 cases considered for Profile-A, only slight deviations in q with respect to the values obtained with a calibrated Manning coefficient were observed (Figure 6a). In fact, in most of the cases, n_A calibrated and n_A calculated were equal and therefore resulted in the same value for q . For the cases where the calculated Manning coefficient did not fully agree with the calibrated Manning coefficient, the differences in q did not exceed $3 l/s/m$ in most cases. Only case 3, 6 and 7 showed larger differences in q of 5.1, 9.1 and $4 l/s/m$, respectively. When q obtained with the calculated Manning simulations was compared with the values of NN_OVERTOPPING2, the differences were larger. For instance, cases 1, 5 and 11 showed deviations in q of $>10 l/s/m$ and case 6 differed in about $9 l/s/m$ (Figure 6b), while the maximum discharge estimated by NN_OVERTOPPING2 was $160 l/s/m$. The RMSE between q simulated by SWASH using the calculated Manning coefficient and calibrated Manning coefficient was $3.13 l/s/m$. In comparison, the RMSE between q simulated by NN_OVERTOPPING2 and q simulated by SWASH using the calculated Manning coefficient was $12.48 l/s/m$.

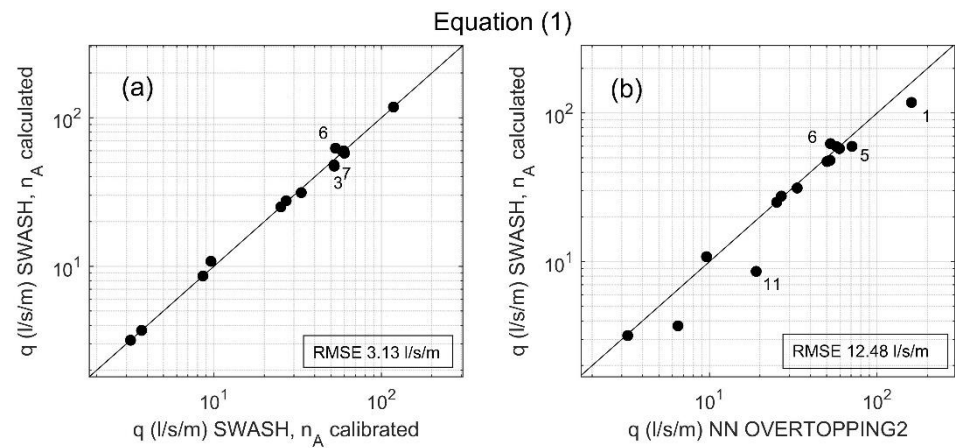


Figure 6. Profile-A. Comparison of q estimated by SWASH using the calculated Manning coefficient by Equation (1) with q estimated by SWASH using the calibrated coefficient (a) and with q estimated by NN_OVERTOPPING2 (b).

3.2. Profile-T

After calibration, the estimations of mean overtopping discharge by SWASH for Profile-T fairly matched the ones obtained by NN_OVERTOPPING2 in most of the 24 cases (see Appendix A, Table A2), that had values ranging from 0.13 to 59 l/s/m. For most cases, the difference between q simulated by SWASH and by NN_OVERTOPPING2 did not exceed 3 l/s/m. For a few cases (8, 15, 20), however, q computed by SWASH was much lower than the one estimated by NN_OVERTOPPING2 (with deviations up to 44 l/s/m). For those cases, during the calibration process, the Manning coefficient could not be decreased further to improve the result for q as it had already reached the established lower limit of $0.02 \text{ s}/(\text{m}^{1/3})$. The remaining cases showed a maximum difference of 3 l/s/m. The RMSE between q simulated by NN_OVERTOPPING2 and by SWASH was of 10.49 l/s/m.

For the development of the Manning coefficient expression, no clear correlation between the Manning coefficient and S_{op} or R_c/H_s was found for the 24 cases simulated with incident wave angles higher than 15° (Figure 7a). However, an inverse relation between q and R_c/H_s could be observed, where for a specific wave steepness, q decreased with increasing R_c/H_s (Figure 7b).

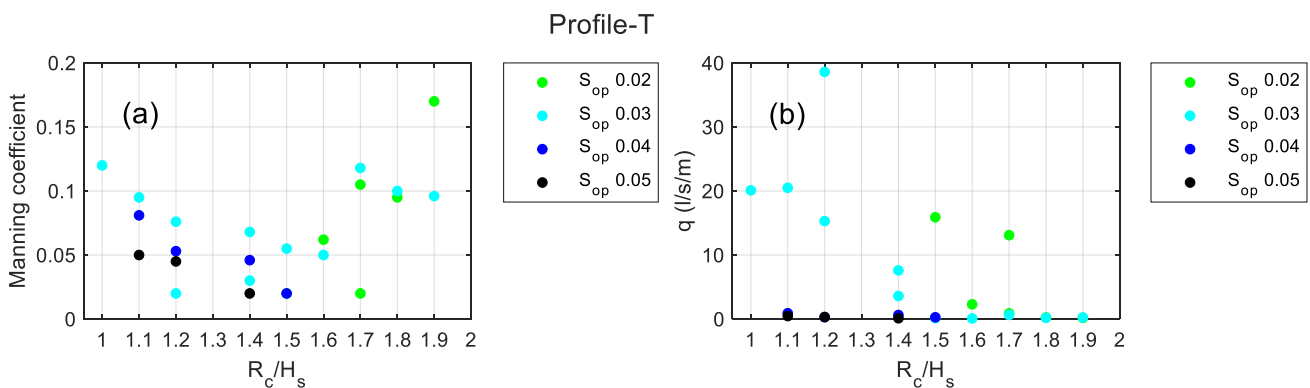


Figure 7. Profile-T. Relation between the Manning coefficient and R_c/H_s (a) and q and R_c/H_s (b).

During these storms, the incident wave angle was related with S_{op} (Figure 8). Cases with high incident waves angles (low $\cos(\beta)$) had mostly higher values of wave steepness, while cases with lower incident wave angles tended to have a lower steepness.

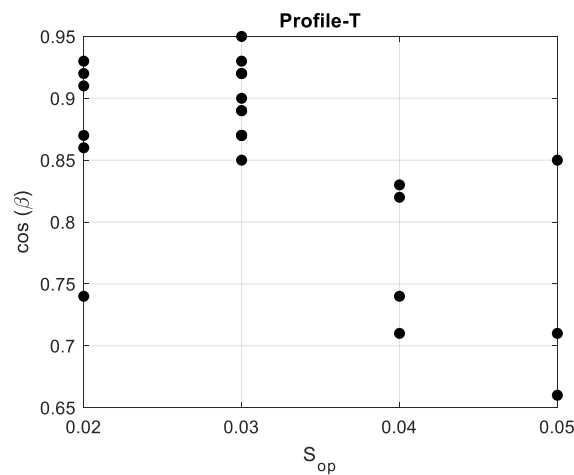


Figure 8. Profile-T. Relation between $\cos(\beta)$ and S_{op} .

Thus, three empirical equations of the Manning coefficient for an armour layer of tetrapods were developed: Equation (2), based on all 24 cases and accounting for the oblique wave attack between 15° and 50° , was developed as a function of the dimensionless crest freeboard R_c/H_s and $\cos(\beta)$. Since the latter was highly related to the wave steepness, S_{op} was not included in the equation and the cosine of the incident wave angle was considered as it displayed higher variability than wave steepness (only four values). This higher variability contributed to the development of the empirical equation. In order to investigate whether the calculated Manning coefficients could achieve a better agreement with the calibrated Manning coefficients when the test cases are separated into two different wave climates, two more equations were developed that can be used alternatively. Equation (3) was based on the 12 simulations of wave climate 1 and accounted for β between 15° and 30° , and Equation (4) was based on the 12 simulations of wave climate 2 and accounted for β between 30° and 50° . Both equations were developed as a function of wave steepness and the dimensionless crest freeboard. The equations of the Manning coefficients $n_{T\ oblique}$, $n_{T\ oblique(15-30)}$ and $n_{T\ oblique(30-50)}$ ($s/(m^{1/3})$) were given as follows:

$$n_{T\ oblique} = a_1 + a_2 \times Rc/Hs + a_3 \times \cos(\beta) + a_4 \times (Rc/Hs)^2 + a_5 \times Rc/Hs \times \cos(\beta) + a_6 \times \cos(\beta)^2 \tag{2}$$

where $a_1 = 1.655$; $a_2 = -0.738$; $a_3 = -2.827$; $a_4 = 0.3895$; $a_5 = -0.4065$; $a_6 = 2.114$

$$n_{T\ oblique(15-30)} = a_1 + a_2 \times Rc/Hs + a_3 \times S_{op} + a_4 \times (Rc/Hs)^2 + a_5 \times Rc/Hs \times S_{op} + a_6 \times (Rc/Hs)^3 + a_7 \times (Rc/Hs)^2 \times S_{op} \tag{3}$$

with $a_1 = -12.96$; $a_2 = 15.26$; $a_3 = 460.3$; $a_4 = -4.398$; $a_5 = -548.2$; $a_6 = -0.03234$; $a_7 = 162.9$

$$n_{T\ oblique\ (30-50)} = a_1 + a_2 \times Rc/Hs + a_3 \times S_{op} + a_4 \times (Rc/Hs)^2 + a_5 \times Rc/Hs \times S_{op} + a_6 \times S_{op}^2 + a_7 \times (Rc/Hs)^3 + a_8 \times (Rc/Hs)^2 \times S_{op} + a_9 \times Rc/Hs \times S_{op}^2 + a_{10} \times S_{op}^3 \tag{4}$$

being $a_1 = 2.617$; $a_2 = -11.47$; $a_3 = 188.8$; $a_4 = 7.496$; $a_5 = 66.13$; $a_6 = -5562$; $a_7 = -1.312$; $a_8 = -49.98$; $a_9 = 686.7$; $a_{10} = 3.756 \times 10^4$.

As these equations were developed under different regimes—they have different ranges of applicability (see Appendix B, Figure A2). While Equation (2) could be used for R_c/H_s ranging between 1.0 and 1.9 and $\cos(\beta)$ ranging between 0.6 and 1.0, Equations (3) and (4) had lower ranges of applicability. For the former, R_c/H_s was between 1.0 and 1.8 and S_{op} between 0.02 and 0.03, and for the latter, R_c/H_s varied between 1.1 and 1.9 and S_{op} between 0.02 and 0.05.

The Manning coefficients that were calculated with Equation (2) showed differences from the calibrated Manning coefficients. While a few values were close or equal, others

differed by $0.02 \text{ s}/(\text{m}^{1/3})$ or more (Figure 9a). The RMSE between the 24 calibrated n_T and calculated $n_{T \text{ oblique}}$ was $0.02 \text{ s}/(\text{m}^{1/3})$, with the largest discrepancies shown in the lowest values. When separating in wave climates, Equation (3) showed better skills to predict the calibrated Manning coefficients than the coefficients obtained for the same cases by Equation 2 (Figure 9b). A RMSE of $0.012 \text{ s}/(\text{m}^{1/3})$ was found between the calibrated and calculated Manning coefficients with Equation (3). The calculated Manning coefficients obtained with Equation (4) also showed a good agreement with the calibrated Manning coefficients (Figure 9c). The RMSE calculated between the calibrated and calculated Manning coefficients with Equation (4) was $0.006 \text{ s}/(\text{m}^{1/3})$ exhibiting the lowest value among the three derived equations.

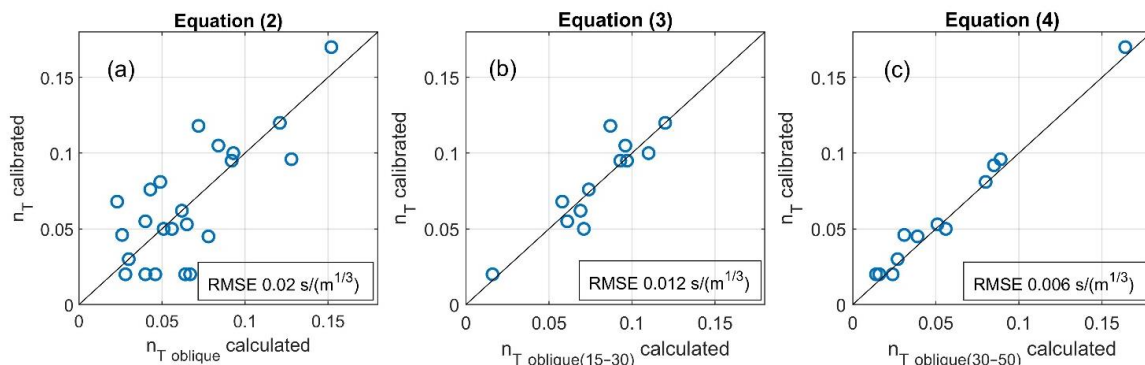


Figure 9. Comparison of calibrated Manning coefficients ($\text{s}/(\text{m}^{1/3})$) with the ones calculated with Equations (2) (a), (3) (b) and (4) (c).

To verify the performance of Equations (2)–(4), the calculated Manning coefficients were applied to simulate overtopping discharges with the SWASH model for the same cases considered during the calibration phase. When comparing the overtopping discharges computed with the calibrated (n_T calibrated) and the calculated ($n_{T \text{ oblique}}$) Manning coefficients by Equation (2), it was found that for the cases of lower discharge, q simulated with $n_{T \text{ oblique}}$ was generally overestimated when compared to q simulated with n_T calibrated (Figure 10a). The RMSE between q simulated by SWASH with the calibrated Manning coefficients and with the calculated Manning coefficients was 1.53 l/s/m . Furthermore, it could be seen that q simulated with $n_{T \text{ oblique}}$ showed slightly larger deviations when compared to the values given by NN_OVERTOPPING2. Generally, overtopping was overestimated in the range of lower discharges, and underestimated in the range of higher discharges (Figure 10b). The RMSE between q simulated by SWASH with $n_{T \text{ oblique}}$ and q computed by NN_OVERTOPPING was 10.62 l/s/m .

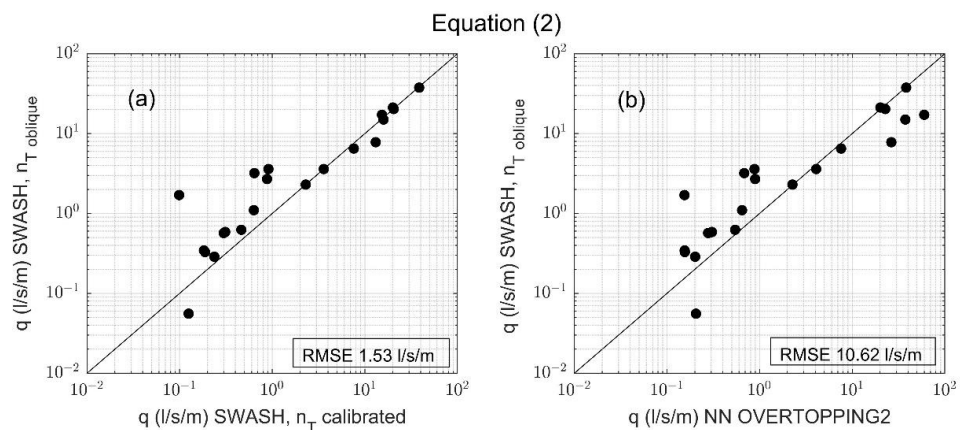


Figure 10. Comparison of q estimated by SWASH using the calculated Manning coefficient by Equation 2 with (a) q estimated by SWASH using the calibrated coefficient and (b) with q estimated by NN_OVERTOPPING2.

The overtopping discharges obtained with the calculated Manning coefficient from Equation (3) ($n_{T\text{ oblique}(15-30)}$) showed a close fit with n_T calibrated (RMSE 1.3 l/s/m) (Figure 11a). In fact, only one case (case 2 in Table 3) resulted in an important deviation (4 l/s/m), while the rest showed deviations of less than 2 l/s/m. The comparison of q computed by NN_OVERTOPPING2 and SWASH with the $n_{T\text{ oblique}(15-30)}$ revealed that both discharges were similar (Figure 11b). Only one case showed a difference of 12 l/s/m (case 15). The RMSE between q estimated by SWASH with the calculated Manning coefficients and the q of NN_OVERTOPPING2 was 6.28 l/s/m. Regarding Equation (4), the results for q obtained by the simulations with $n_{T\text{ oblique}(30-50)}$ matched closely the discharge obtained with n_T calibrated (RMSE = 0.59 l/s/m) (Figure 11c). The discharges for this wave climate were generally low (most cases had discharges of < 1 l/s/m). The highest deviation found between q simulated with a calibrated Manning and q simulated with a calculated Manning was of 1.9 l/s/m. Comparing the SWASH simulated discharges with $n_{T\text{ oblique}(30-50)}$, with the values of NN_OVERTOPPING2, a larger RMSE was found (13.46 l/s/m) (Figure 11d). The two cases that were responsible for this large error were cases 8 and 20 in Table 3, with discharges of 60 and 26 l/s/m, respectively, where SWASH showed deviations of 45 and 13 l/s/m in regard to q computed by NN_OVERTOPPING2.

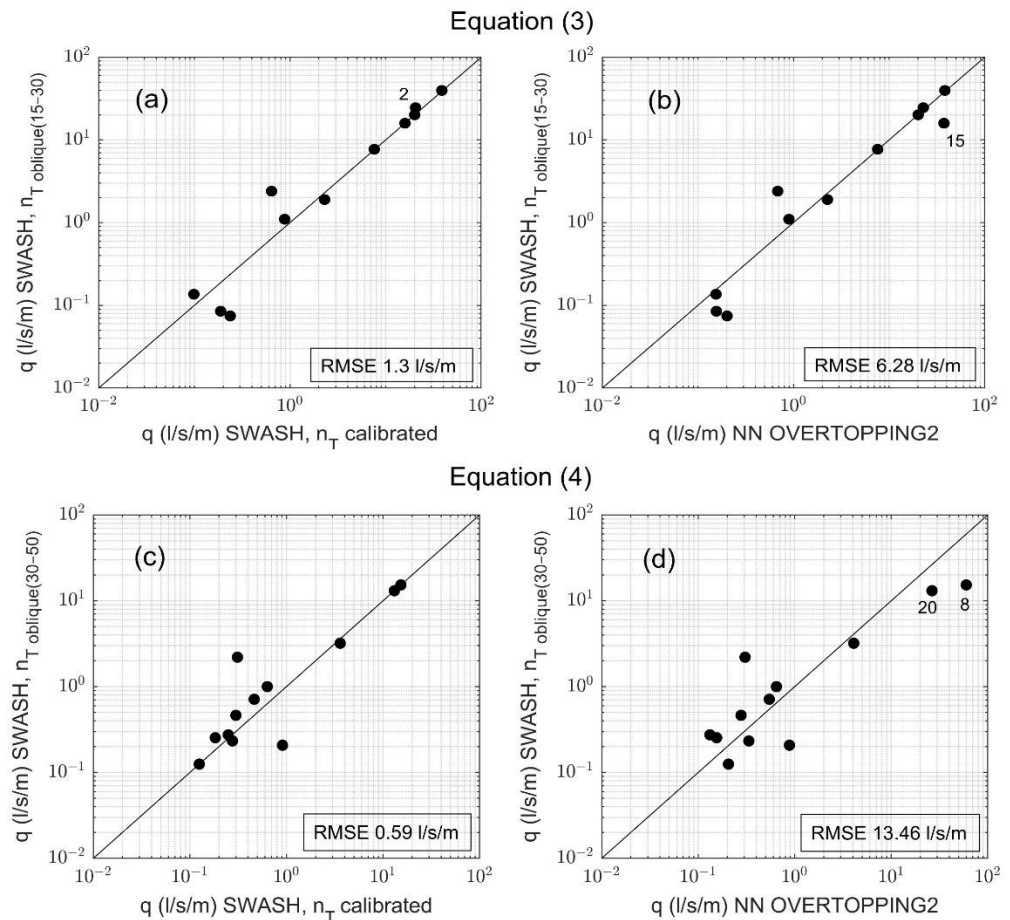


Figure 11. Comparison of q estimated by SWASH using $n_{T\text{ oblique}(15-30)}$ with (a) q estimated by SWASH using the n_T calibrated and with (b) q estimated by NN_OVERTOPPING2, and of q estimated by SWASH using $n_{T\text{ oblique}(30-50)}$ with (c) q estimated by SWASH using n_T calibrated and with (d) q estimated by NN_OVERTOPPING2.

4. Discussion

The overtopping simulations at Ericeira harbour demonstrated that the SWASH model is capable of providing similar results as the neural network tool NN_OVERTOPPING2 when the value for bottom friction of the armour layer is calibrated, even for different profile

morphologies and typologies. However, in some cases where the Manning coefficient was limited to $0.02 \text{ s}/(\text{m}^{1/3})$, the discharge was lower in the SWASH simulations than in the NN_OVERTOPPING2 tool. A similar issue was observed by [30], who found that the model clearly underestimated the overtopping discharge for complex structure types. They suggested that the velocity of overtopped water masses is underestimated because the velocity differences in front of the structure between bottom and surface were not well described by the model in simulations with one vertical layer. Furthermore, previous studies have shown that the accuracy of the SWASH model can depend on the model settings. For example, according to [17], the estimation of mean overtopping discharge appears to be sensitive to the non-dimensional parameter L/dx (wavelength at the toe of the structure over grid size). Based on calculations performed by [31], however, this sensitivity could not be confirmed (Appendix C, Figures A3 and A4).

In addition, for the evaluation of the performance of SWASH, it must be recalled that the results obtained by SWASH were not validated with real data, but with another tool for the estimation of overtopping. In order to confirm if it is indeed the SWASH model that underpredicts, or possibly NN_OVERTOPPING2 that overpredicts, real data are necessary to compare the results and draw a conclusion. While the neural network is a commonly used tool to perform the overtopping predictions, the SWASH model shows some advantages in the use for operational systems like HIDRALERTA, as mentioned in Section 1, namely the capability to estimate the flood extension or the flooded area by implementing a 2D model. Especially for studies where the wave propagation plays an important role, SWASH, in contrast to NN_OVERTOPPING2, is able to extract wave characteristics travelling through the domain at any given point.

During the model calibration for Profile-A, a RMSE of 12.11 l/s/m was obtained between the simulated mean overtopping discharge by SWASH and the one by NN_OVERTOPPING2. It must be noted here, however, that the discharges computed by NN_OVERTOPPING2 were generally very high (maximum discharge 160 l/s/m). The impact of the inaccuracy of q predictions depends on the kind of receptor that is considered in the Early Warning System. An overtopping discharge of 3 l/s/m may not cause severe erosion or damage at the structure but can be harmful for pedestrians.

The model calibration for Profile-T included a large variety of cases with different wave characteristics, but the values for q estimated by NN_OVERTOPPING2 could be matched closely in most cases by SWASH. The RMSE between the values of both models was 10.49 l/s/m , although as observed at Profile-A, only a few cases, where q was underestimated by SWASH by $> 10 \text{ l/s/m}$, were responsible for this high error.

For the development of the Manning coefficient expressions, the results partially confirmed the findings of [21], who found a correlation between the Manning coefficient, R_c/H_s and S_{op} . However, this correlation could only be observed when the angle of wave attack was considered. At this point, it must be noted that the work of [21] was performed under controlled conditions, while in this study, real storm events were used, which makes the model calibration more demanding. The fact that the simulations not only included large ranges of wave periods and wave heights, but also incident wave angles between 15° and 50° degrees can make it difficult to find these relations between R_c/H_s and S_{op} . Many studies have shown that wave obliquity has an impact on overtopping estimation (e.g., [16,29]). As the developed expressions are based exclusively on the wave conditions during real storm events in Ericeira, the ranges of applicability presented in Appendix B are of great importance to the use of these expressions. Once the input conditions for the SWASH model lie outside of these ranges, the expressions will not produce reliable results and are therefore not applicable.

Due to the relatively high root-mean-square error of the overtopping simulations based on Equation (2), the simulated cases were analysed and separated into two different wave conditions according to their wave characteristics. Thus, it was possible to investigate whether also the behaviour of the Manning coefficient was related to these wave characteristics.

The equations that resulted from the separation of the simulations of this profile resulted in very small errors for the calculation of the Manning coefficient in comparison to the ones obtained by Equation (2). At this point, it must be noted that the relevance of the RMSE error estimations reduces, once the number of calibration data and the amount of coefficients in the expression become similar, as in Equations (3) and (4), which are based on only a few test cases. The reduction in RMSE was $0.008 \text{ s}/(\text{m}^{1/3})$ for Equation (3) and $0.014 \text{ s}/(\text{m}^{1/3})$ for Equation (4). This showed that, by dividing the cases according to their wave direction and characteristics, the performance of the equations could be improved but will have to be validated with more data in future studies. Although each equation consequently had a smaller range of applicability, their combined use can overcome this constraint. This indicates that there might not only be a correlation between the Manning coefficient, R_c/H_s and S_{op} , but also a possible dependency of the Manning coefficient on the incident wave angle. This dependency can be explained by the fact that an oblique wave attack reduces the overtopping discharge estimated by NN_OVERTOPPING2 and the way that the calibrated SWASH model can replicate this is with an increased Manning friction coefficient, causing a decrease in overtopping discharge. Overall it can be said that these findings suggest to implement Equation (3) and (4), rather than Equation (2), as they showed a better performance with smaller errors and will most likely deliver more reliable results.

For the implementation of SWASH into an operational system like HIDRALERTA, the model run time has to be considered. The simulations were performed on a Windows operating system with Intel Core i5-1035G1 (CPU 1,0 GHz, 4 cores). SWASH was run serial, using one processor, and took approximately 10 min for each simulation. NN_OVERTOPPING2, however, shows a lower model run time of only a few seconds.

5. Conclusions

This study was conducted to investigate the capabilities of SWASH to be integrated into the HIDRALERTA Early Warning System by calibrating two one-dimensional models for storm conditions at the Ericeira harbour prototype and developing an expression for the definition of the Manning coefficient of different armour layers of the breakwater based on the sea wave conditions.

The calibration of the one-dimensional model for Profile-A (antifer cubes) and Profile-T (tetrapods) for the Ericeira harbour demonstrated that, in this study, the SWASH model performance for the estimation of mean overtopping discharge is strongly governed by the Manning coefficient. With a calibrated Manning coefficient, the model is capable of providing similar results than with NN_OVERTOPPING2 at a low computational effort. Nevertheless, in some cases, the SWASH model still underpredicted the overtopping discharge.

The simulations revealed that the variables R_c/H_s and S_{op} , which were considered in this study, are important variables defining the Manning coefficient and that, for the development of an expression for the Manning coefficient, the angle of wave attack must be considered. Thus, the incident wave angles must be included as an independent variable in the formula in the form of the cosine of the incident angle. Alternatively, the simulations that are used to develop the Manning coefficient expressions can be separated, based on their incident wave angles. Therefore, it is possible to account for wave obliquity as it cannot specifically be included in one-dimensional simulations in SWASH. For the implementation into HIDRALERTA, the ranges of application of the developed expression are fundamental, as they will not produce reliable results in situations where the values of the wave conditions lie outside of these ranges. In those cases, the results for mean overtopping discharge will solely be based on the estimations by NN_OVERTOPPING2.

As a final conclusion and in the framework of this study, it can be said that the SWASH model is capable of providing reasonable results and it has the potential to be implemented in the Early Warning System HIDRALERTA. However, the type of receptor that is considered in the risk assessment plays an important role when assessing the performance of the SWASH model for the Ericeira prototype. The discrepancies of simulated mean overtop-

ping discharge with the ones estimated by NN_OVERTOPPING2 are significant in the case of a risk assessment for pedestrians and have to be improved if the SWASH model was to be implemented in HIDRALERTA. Generally, after calibration, SWASH mostly delivers reliable results at a low computational cost (for its one-dimensional version). Nevertheless, in order to make a final statement on the performance of SWASH, the results have to be compared against field data. In addition, SWASH is capable of modelling the wave propagation as well as the overtopping process, allowing for a future definition of the extension of the flooded area, which cannot be accomplished with tools like NN_OVERTOPPING2. The development of expressions to seamlessly calculate the Manning coefficient helped to build the frame for the SWASH implementation in HIDRALERTA system as an alternative to the neural network NN_OVERTOPPING2.

Author Contributions: Conceptualisation, methodology, writing—original draft preparation, A.M.; review, editing and supervision, A.C.Z. and J.L.G.; project administration, A.C.Z. All authors have read and agreed to the published version of the manuscript.

Funding: This research was supported by the Portuguese Foundation of Science and Technology (FCT) under the project LA/P/0069/2020 granted to the Associate Laboratory ARNET and UID/00350/2020 CIMA and by the research project BSafe4Sea (Ref. PTDC/ECI-EGC/31090/2017).

Institutional Review Board Statement: Not applicable.

Informed Consent Statement: Not applicable.

Acknowledgments: The authors acknowledge the research projects To-SEAlert (Ref. PTDC/EAM-OCE/31207/2017), BSafe4Sea (Ref. PTDC/ECI-EGC/31090/2017) and EW-COAST (Ref. ALG-LISBOA-01-145-FEDER-028657, with financial support of FCT under the project LA/P/0069/2020 granted to the Associate Laboratory ARNET and UID/00350/2020 CIMA). Infraestrutura Nacional de Computação Distribuída (INCD) is also acknowledged for the access to their computational resources, as well as Copernicus program.

Conflicts of Interest: The authors declare no conflict of interest.

Appendix A

Results for mean overtopping discharge obtained by NN_OVERTOPPING2 and by SWASH and values of the calibrated Manning coefficients

Table A1. Estimated overtopping Profile-A.

Case No	q (l/s/m) NN_OVERTOPPING2	q (l/s/m) SWASH	Manning Coefficient Calibrated (s/(m ^{1/3}))
1	160.42	117.91	0.02
2	59.64	60.14	0.07
3	50.33	52.34	0.07
4	57.42	58.50	0.08
5	70.88	59.72	0.02
6	52.72	53.20	0.06
7	52.37	52.11	0.04
8	33.38	33.24	0.06
9	25.19	25.14	0.04
10	26.85	27.02	0.05
11	19.01	8.60	0.02
12	9.61	9.62	0.03
13	6.49	3.74	0.02
14	3.26	3.18	0.06

Table A2. Estimated overtopping Profile-T.

Case No	q (l/s/m) NN_OVERTOPPING2	q (l/s/m) SWASH	Manning Coefficient Calibrated (s/(m ^{1/3}))
1	20.14	20.14	0.12
2	22.74	20.52	0.10
3	0.54	0.46	0.05
4	0.88	0.91	0.08
5	0.31	0.31	0.05
6	0.28	0.30	0.05
7	38.26	38.64	0.08
8	59.93	15.33	0.02
9	0.21	0.13	0.02
10	0.65	0.63	0.05
11	7.58	7.60	0.07
12	4.09	3.60	0.03
13	0.33	0.28	0.02
14	0.17	0.14	0.06
15	37.48	15.94	0.02
16	0.15	0.10	0.05
17	2.26	2.34	0.06
18	0.68	0.64	0.12
19	0.90	0.88	0.11
20	26.44	13.14	0.02
21	0.16	0.19	0.10
22	0.20	0.22	0.10
23	0.13	0.25	0.10
24	0.16	0.18	0.17

Appendix B

Ranges of application for the developed equations.

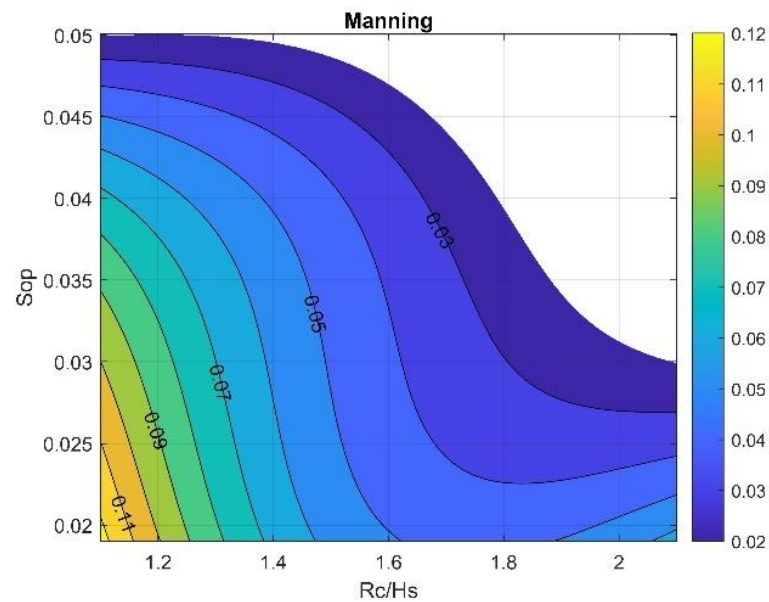


Figure A1. Profile-A. Range of application of Equation (1).

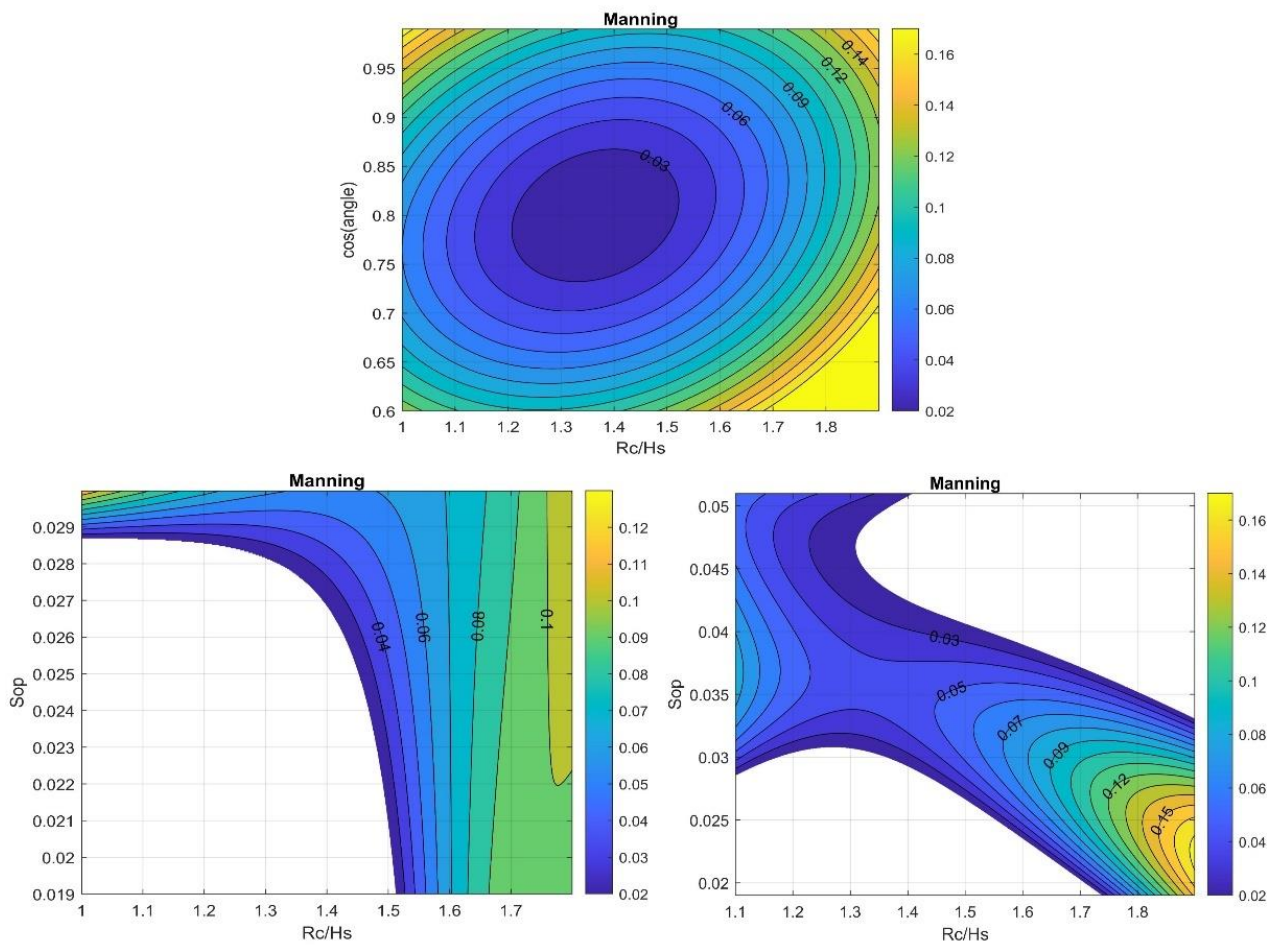


Figure A2. Profile-T. Range of application of Equations 2 (top), 3 (bottom left) and 4 (bottom right).

Appendix C

Correlations of mean overtopping discharge estimations and L/dx

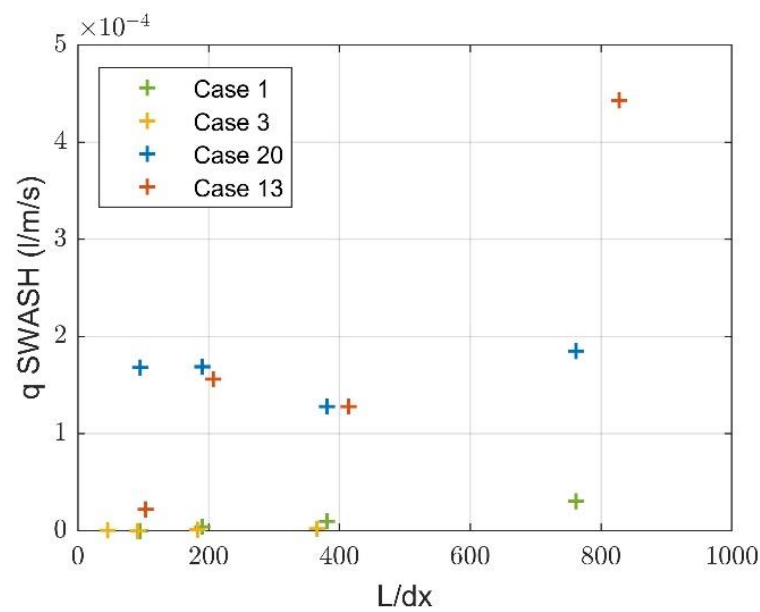


Figure A3. Relation of the mean overtopping discharge versus L/dx based on the calculations of [31].

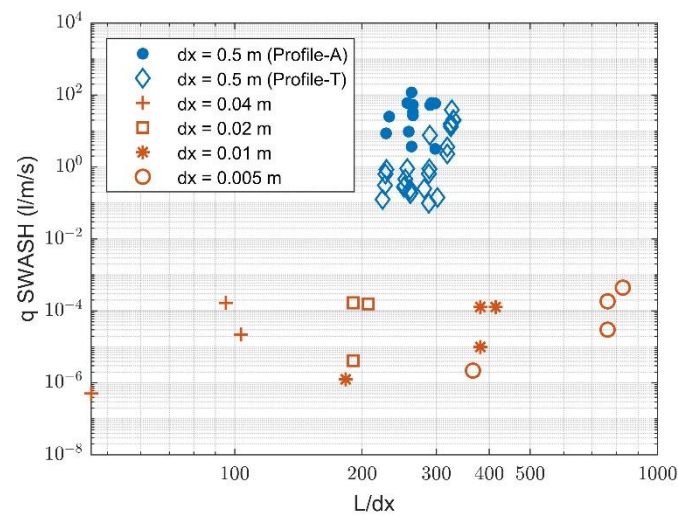


Figure A4. Ratio of the mean overtopping discharge versus L/dx based on the calculations of [31] and the cases of this study.

References

1. Tavares, A.O.; Barros, J.L.; Freire, P.; Santos, P.P.; Perdiz, L.; Fortunato, A.B. A Coastal Flooding Database from 1980 to 2018 for the Continental Portuguese Coastal Zone. *Appl. Geogr.* **2021**, *135*, 102534. [\[CrossRef\]](#)
2. Fortes, C.; Reis, M.T.; Poseiro, P.; Capitão, R.; Santos, J.; Pinheiro, L.; Craveiro, J.; Rodrigues, A.; Sabino, A.; Ferreira Silva, S.; et al. HIDRALERTA Project—A Flood Forecast and Alert System in Coastal and Port Areas. In Proceedings of the IWA – World Water Congress & Exhibition, Lisbon, Portugal, 21–26 September, 2014. [\[CrossRef\]](#)
3. Pillai, K.; Etemad-Shahidi, A.; Lemckert, C. Wave Overtopping at Berm Breakwaters: Review and Sensitivity Analysis of Prediction Models. *Coast. Eng.* **2017**, *120*, 1–21. [\[CrossRef\]](#)
4. Lavell, A.; Oppenheimer, M.; Diop, C.; Hess, J.; Lempert, R.; Li, J.; Muir-Wood, R.; Myeong, S.; Moser, S.; Takeuchi, K.; et al. Climate Change: New Dimensions in Disaster Risk, Exposure, Vulnerability, and Resilience. In *Managing the Risks of Extreme Events and Disasters to Advance Climate Change Adaptation*; Field, C.B., Barros, V., Stocker, T.F., Dahe, Q., Eds.; Cambridge University Press: Cambridge, UK, 2012; pp. 25–64. [\[CrossRef\]](#)
5. van Dongeren, A.; Ciavola, P.; Martinez, G.; Viavattene, C.; Bogaard, T.; Ferreira, O.; Higgins, R.; McCall, R. Introduction to RISC-KIT: Resilience-Increasing Strategies for Coasts. *Coast. Eng.* **2018**, *134*, 2–9. [\[CrossRef\]](#)
6. Gracia, V.; García-León, M.; Sánchez-Arcilla, A.; Gault, J.; Oller, P.; Fernández, J.; Sairouni, A.; Cristofori, E.; Toldrà, R. A new generation of early warning systems for coastal risk. the icoast project. *Coast. Eng. Proc.* **2014**, *1*, 1–8. [\[CrossRef\]](#)
7. Poseiro, P. *Forecast and Early Warning System for Wave Overtopping and Flooding in Coastal and Harbour Areas: Development of a Model and Risk Assessment*; IST-UNL: Lisbon, Portugal, 2019.
8. Fortes, C.J.E.M.; Reis, M.T.; Pinheiro, L.; Poseiro, P.; Serrazina, V.; Mendonça, A.; Smithers, N.; Santos, M.I.; Barateiro, J.; Azevedo, E.B.; et al. The HIDRALERTA System: Application to the Ports of Madalena Do Pico and S. Roque Do Pico, Azores. *Aquat. Ecosyst. Health Manag.* **2020**, *23*, 398–406. [\[CrossRef\]](#)
9. Pinheiro, L.; Fortes, C.J.E.M.; Reis, M.T.; Santos, J.; Soares, C.G. Risk Forecast System for Moored Ships. *Vicce Virtual Int. Conf. Coast. Eng.* **2020**, *36*, 37. [\[CrossRef\]](#)
10. Santos, M.I.; Pinheiro, L.; Fortes, J.C.E.M.; Reis, M.T.; Serrazina, V.; Azevedo, E.B.; Reis, F.V.; Salvador, M. Simulation of Hurricane Lorenzo at the Port of Madalena Do Pico, Azores, by Using the HIDRALERTA System. In Proceedings of the MARTECH 5th International Conference on Maritime Technology and Engineering, Lisbon, Portugal, 16–19 November 2020.
11. Zózimo, A.C.; Ferreira, A.M.; Pinheiro, L.; Fortes, C.J.E.; Baliko, M. Implementação Do Sistema HIDRALERTA Para a Zona Costeira Da Costa Da Caparica. In Proceedings of the X Congresso sobre Planeamento e Gestão das Zonas Costeiras dos Países de Expressão Portuguesa, Rio de Janeiro, Brazil, 6–10 December 2021.
12. Coeveld, E.M.; Van Gent, M.R.A.; Pozueta, B. *Neural Network Manual for NN_Overtopping Program*; Technical Report, TU Delft: Delft, The Netherlands, 2005.
13. Fortes, C.J.E. Transformações Não-Lineares de Ondas Marítimas Em Zonas Portuárias. Análise Pelo Método Dos Elementos Finitos. Ph.D. Thesis, Laboratório Nacional de Engenharia Civil, Lisboa, Portugal, 2002.
14. Flater, D. Xtide. Available online: <https://flaterco.com/xtide> (accessed on 15 December 2021).
15. Tonelli, M.; Petti, M. Numerical Simulation of Wave Overtopping at Coastal Dikes and Low-Crested Structures by Means of a Shock-Capturing Boussinesq Model. *Coast. Eng.* **2013**, *79*, 75–88. [\[CrossRef\]](#)

16. EurOtop. *Manual on Wave Overtopping of Sea Defences and Related Structures. An Overtopping Manual Largely Based on European Research, but for Worldwide Application.*; Van der Meer, J.W., Allsop, N.W.H., Bruce, T., De Rouck, J., Kortenhaus, A., Pullen, T., Schüttrumpf, H., Troch, P., Zanuttigh, B., Eds. EurOtop. 2018. Available online: <http://www.overtopping-manual.com> (accessed on 15 December 2021).
17. Suzuki, T.; Altomare, C.; Veale, W.; Verwaest, T.; Trouw, K.; Troch, P.; Zijlema, M. Efficient and Robust Wave Overtopping Estimation for Impermeable Coastal Structures in Shallow Foreshores Using SWASH. *Coast. Eng.* **2017**, *122*, 108–123. [[CrossRef](#)]
18. Zijlema, M.; Stelling, G.; Smit, P. SWASH: An Operational Public Domain Code for Simulating Wave Fields and Rapidly Varied Flows in Coastal Waters. *Coast. Eng.* **2011**, *58*, 992–1012. [[CrossRef](#)]
19. Suzuki, T.; Verwaest, T.; Veale, W.; Trouw, K.; Zijlema, M. A numerical study on the effect of beach nourishment on wave overtopping in shallow foreshores. *Coast. Eng. Proc.* **2012**, *1*. [[CrossRef](#)]
20. Suzuki, T.; Altomare, C.; Verwaest, T.; Trouw, K.; Zijlema, M. Two-dimensional wave overtopping calculation over a dike in shallow foreshore by swash. *Coast. Eng. Proc.* **2014**, *1*, Structures.3. [[CrossRef](#)]
21. Zhang, N.; Zhang, Q.; Wang, K.-H.; Zou, G.; Jiang, X.; Yang, A.; Li, Y. Numerical Simulation of Wave Overtopping on Breakwater with an Armor Layer of Accropode Using SWASH Model. *Water* **2020**, *12*, 386. [[CrossRef](#)]
22. Celli, D.; Pasquali, D.; De Girolamo, P.; Di Risio, M. Effects of Submerged Berms on the Stability of Conventional Rubble Mound Breakwaters. *Coast. Eng.* **2018**, *136*, 16–25. [[CrossRef](#)]
23. Liang, B.; Wu, G.; Liu, F.; Fan, H.; Li, H. Numerical Study of Wave Transmission over Double Submerged Breakwaters Using Non-Hydrostatic Wave Model. *Oceanologia* **2015**, *57*, 308–317. [[CrossRef](#)]
24. Hersbach, H.; Bell, B.; Berrisford, P.; Biavati, G.; Horányi, A.; Muñoz Sabater, J.; Nicolas, J.; Peubey, C.; Radu, R.; Rozum, I.; et al. *ERA5 Hourly Data on Single Levels from 1959 to Present*; Copernicus Climate Change Service (C3S) Climate Data Store (CDS): Reading, UK, 2018. [[CrossRef](#)]
25. Swan Team. *Swan User Manual, 40.51.*; Department of Civil Engineering and Geosciences, Delft university of Technology: Delft, The Netherlands, 2006.
26. Pés, V.M. *Applicability and Limitations of the SWASH Model to Predict Wave Overtopping*; TU Delft: Delft, The Netherlands; Universitat Politècnica de Catalunya: Barcelona, Spain, 2013.
27. Salas Pérez, M. *Overtopping over a Real Rubble Mound Breakwater Calculated with SWASH*; Universitat Politècnica de Catalunya: Barcelona, Spain; Delft University of Technology: Delft, The Netherlands, 2014.
28. TAW. *Technisch Rapport Golfploop En Golfoverslag Bij Dijken (Technical Report on Wave Run-up and Wave Overtopping at Dikes—In Dutch)*; Technical Advisory Committee on Flood Defence: Brussels, Belgium, 2002.
29. Galland, J.C. Rubble mound breakwater stability under oblique waves: And experimental study. *Coast. Eng. Proc.* **1994**, *1*, 24. [[CrossRef](#)]
30. Vanneste, D.F.A.; Altomare, C.; Suzuki, T.; Troch, P.; Verwaest, T. Comparison of numerical models for wave overtopping and impact on a sea wall. *Coast. Eng. Proc.* **2014**, *1*, 5. [[CrossRef](#)]
31. Manz, A. *Application of SWASH to Determine Overtopping during Storm Events in the Port of Ericeira and Its Introduction into HIDRALERTA System*; Universidade do Algarve: Faro, Portugal, 2021.